nature immunology

An autonomous CDR3δ is sufficient for recognition of the nonclassical MHC class I molecules T10 and T22 by γδ T cells

Erin J Adams[1], Pavel Strop[2], Sunny Shin[3], Yueh-Hsiu Chien[3] & K Christopher Garcia[2,4]

It remains unclear whether γδ T cell antigen receptors (TCRs) detect antigens in a way similar to antibodies or αβ TCRs. Here we show that reactivity between the G8 and KN6 γδ TCRs and the major histocompatibility complex class Ib molecule T22 could be recapitulated, with retention of wild-type ligand affinity, in an αβ TCR after grafting of a G8 or KN6 complementarity-determining region 3-δ (CDR3δ) loop in place of the CDR3α loop of an αβ TCR. We also found that a shared sequence motif in CDR3δ loops of all T22-reactive γδ TCRs bound T22 in energetically distinct ways, and that T10^{d}, which bound G8 with weak affinity, was converted into a high-affinity ligand by a single point mutation. Our results demonstrate unprecedented autonomy of a single CDR3 loop in antigen recognition.

All γδ T cells express a somatically rearranged T cell receptor (TCR) through which they recognize antigen. These γδ TCRs are composed of a γ- and δ-chain, with a structure generally similar to that of an αβ TCR or the Fab fragment of an antibody[1,2]. Recognition of ligand results in a variety of effector outcomes from γδ T cells, some of which are similar to those of αβ T cells[3–6], such as cytokine secretion and cytotoxic activity[7–9], and others that are more unique to γδ T cells, such as wound repair[10], antigen-presenting activity through expression of major histocompatibility complex (MHC) class II molecules[11] and immunosuppresion[12]. It has been suggested that γδ T cells are effectors in a variety of infectious and autoimmune diseases[13], and some have the ability to spontaneously lyse tumor cells[7,13].

The molecular basis of the recognition of ligand by γδ TCRs is not well understood. Is it more similar to that of an αβ TCR, whereby the germline-encoded variable (V) regions interact with MHC through a coevolved 'bias' and the complementarity-determining region 3 (CDR3) regions recombine uniquely to 'read out' different antigenic peptides[14,15]? Or is γδ TCR ligand recognition more similar to that of antibody-antigen interactions, in which there is presumably no antigen bias and a combination of somatic hypermutation and CDR3 recombination enables reactivity with a 'universe' of antigens[16]? In both cases, interactions are usually mediated by simultaneous contact of multiple CDR loops of the antigen receptor with the antigen, with variable contributions of CDR involvement among different complexes. Also, in both cases, the recombined CDR3-H and CDR3β loops exert a general dominance during ligand recognition by antibodies and αβ TCRs, respectively, as measured by the extent of contact.

Much effort has been spent trying to identify the ligands for γδ TCRs, yet only a few are well defined. These include MHC class Ib molecules (CD1c[4,17], T10 and T22 (refs. 18,19), MICA[20] and H2 I-E^{k} (ref. 18)), non–immune system–related proteins (F1 subunit of the ATP synthase[21]) and microbial proteins (herpes simplex virus 1 glycoprotein I; ref. 22). The structural diversity of these ligands suggests that the antigen-recognition process of γδ T cells is unlike that of conventional αβ T cells. Indeed, the genetics of γδ TCR rearrangement suggest that diversity of the CDR1 and CDR2 loops, encoded by the approximately eight V segments of the δ-chain and approximately ten V gene segments of the γ-chain is not extensive. Instead, sequence diversity is concentrated in the rearranged portion of the receptor, specifically the CDR3γ and CDR3δ loops. The ability to use many diversity (D) segments in the rearrangement of the δ-chain[23] endows this loop with the greatest amino acid diversity potential of all the rearranged receptors.

The molecular details of how this unique feature of γδ TCRs is used in antigen recognition remains unclear, except for interactions between T10 and T22 and γδ TCRs. Approximately 0.1–1.0% of mouse γδ T cells recognize the MHC class Ib molecules T10 and T22 (ref. 24). Of this population, G8 (ref. 25) and KN6 (refs. 26,27) are the two best characterized γδ TCRs specific for T10 and T22. The three-dimensional structure of G8 in complex with T22 (ref. 1) provides structural insight into how γδ T cells 'see' antigen and demonstrates a recognition strategy substantially different from that of αβ TCR recognition of peptide-MHC complexes or antibody recognition of antigen. G8 binds T22 almost exclusively through an extended CDR3δ loop, with minor contacts from the remaining CDR loops; the result is

[1]Department of Biochemistry and Molecular Biology, University of Chicago, Chicago, Illinois 60637, USA. [2]Department of Molecular and Cellular Physiology and Department of Structural Biology, [3]Department of Microbiology & Immunology and Program in Immunology, and [4]Howard Hughes Medical Institute, Stanford University School of Medicine, Stanford, California 94305, USA. Correspondence should be addressed to E.J.A. (ejadams@uchicago.edu) or K.C.G. (kcgarcia@stanford.edu).

Received 1 April; accepted 5 May; published online 30 May 2008; doi:10.1038/ni.1620

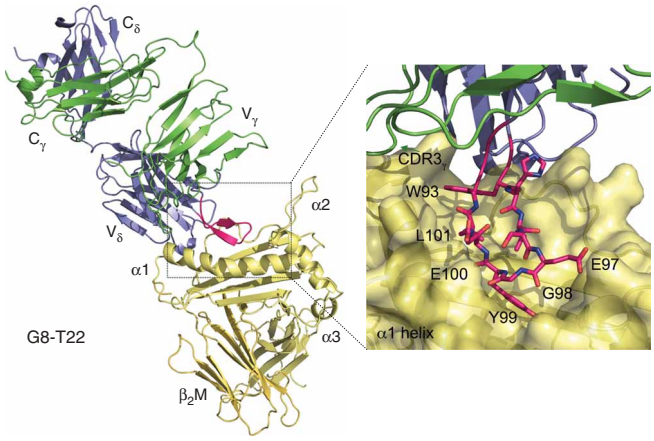

Figure 1 Three-dimensional structure of the G8 γδ TCR in complex with the MHC class Ib molecule T22. Blue, G8 δ-chain; green, G8 γ-chain; yellow, T22; red, G8 CDR3δ loop. β_2M, β_2-microglobulin; C, constant chain. Right, enlargement of the G8 CDR3δ loop (red) in contact with T22 (yellow). The residues of the W…EGYEL motif present in all T22-binding γδ TCRs are labeled at right.

a tilted G8-T22 docking orientation. Other T22-binding γδ TCRs, despite using different V_δ and V_γ domains, are related to G8 by a shared six–amino acid motif (W…EGYEL) in their CDR3δ loops[28]. TCRs using the same V_γ and V_δ but with variation in the number and composition of amino acids between the 'W' and 'EGYEL' portions have been shown, by tetramer decay, to bind T22 with different affinities[28]. In the case of G8, this CDR3δ motif forms extensive interactions with T22 in the complex interface and thus may be the main T22-recognition determinant. However, variation in length and amino acid composition of the intervening residues between the 'W' and 'EGYEL' portions raises the issue of how this variability, generated by the rearrangement process, is accommodated during recognition. The structures of a non–ligand-bound human $V_\delta3$ domain[29] and a human γδ TCR[2] also show protruding CDR3 loops, but the structural ramifications for antigen recognition are not known.

In addition to the variation in the CDR3δ loop of these T10- and T22-reactive γδ TCRs, allelic forms of T10 and T22 are recognized differently. T10 from H-2^d mice ($T10^d$) weakly stimulates the G8 hybridoma, approximately 10% that of T10 and T22 from mice expressing H-2^b. This demonstrates that amino acid variation in these loci can modulate γδ T cell reactivity. The parameters that govern the binding of TCR to $T10^d$ that result in this weak stimulation of G8 and the identity of positions of variation in the H-2^b versus H-2^d versions of T10 and T22 that are critical for stimulation are not known.

Here we undertook a structure-function study to better understand the molecular determinants of the recognition of T10 and T22 molecules by γδ TCRs. We explored the issue of whether the CDR3δ loop is the chief recognition determinant in T22 binding and how variations among receptors in the W…EGYEL motif can modulate binding to T22. We also defined the critical variable residues in T10 and T22 responsible for differential binding by and stimulation of T22-specific γδ TCRs. Our conclusions indicate an unexpected structural autonomy of the TCR CDR3δ loop in ligand recognition and identify a single amino acid substitution in T10 and T22 responsible for ligand specificity.

RESULTS

G8 CDR3δ: minimal T22 recognition determinant

Published results have shown that γδ T cells that recognize T22 contain a variety of V_δ and V_γ domains in their rearranged γδ TCRs[1,28], which indicates the presence of a variety of sequences in their CDR1 and CDR2 loops. However, the feature shared by these TCRs is the W…EGYEL motif assembled by exclusive use of the $D_\delta2$ segment (EGYE) with partial contributions by the V_δ segment (W), the $D_\delta1$ segment (W) and/or P nucleotides (L)[28]. That observation suggests that the main recognition determinant for T22 recognition is in the CDR3δ loop. Structural elucidation of the complex of the G8 γδ TCR with T22 showed that this CDR3δ loop contained most of the recognition interface (67% of the total buried surface area) between G8 and T22 (**Fig. 1**). The sequence motif of this specific CDR3δ (…WHISEGYEL…) formed the principal contacts with the floor of the interhelical groove in T22 (**Fig. 1**). We also noted considerable 'wobble' in the binding orientation of G8 when it was docked with T22. That is, superposition of the T22 molecules in the two complexes in the crystallographic asymmetric unit showed a resultant difference of approximately 6Å between the two TCRs around a structurally invariant CDR3δ pivot point that formed the T22 contact. This suggested that the CDR3δ loop anchored the complex, which allowed the 'body' of the TCR to adopt a range of different positions when bound to T22. The finding that CDR3δ seemed to be the 'glue' holding the complex together led us to hypothesize that the CDR3δ loop alone could endow binding of T22 when 'grafted' onto an alternative structural scaffold.

To test that hypothesis, we grafted the CDR3δ loops of two canonical T22-specific TCRs, G8 and KN6, onto a 'naive' TCR background, that of the 172.10 αβ TCR that binds MHC class II I-A^u bound to acetylated myelin basic protein[30] but not to T22. The availability of the coordinates for both G8 and 172.10 allowed us to design the grafting boundary based on superposition (less than 2 Å r.m.s.d.) of the two structures (**Fig. 2** and **Supplementary Fig. 1** online). We used those structures to visually guide grafting of the CDR3δ loop in place of the 172.10 CDR3α loop such that the graft junctions would be sterochemically reasonable and that it would be presented in a sterically unobstructed way in the context of the αβ TCR framework and binding site (**Supplementary Fig. 1**). In fact, the framework residues at the CDR3 graft junctions (the *f* and *g* strands of

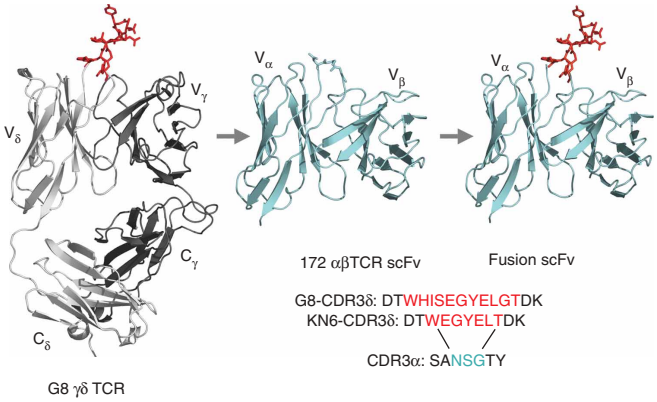

Figure 2 Transfer of CDR3δ onto CDR3α. (**a**) Full-length G8 γδ TCR[1] (left: gray, TCR; red, CDR3δ loop), the 172 αβ TCR single-chain Fv construct (scFv; blue; middle), and the fusion construct (right) with the CDR3δ loop (red) grafted onto the CDR3α loop. Bottom right, sequences of CDR3δ loops grafted from the G8 and KN6 γδ TCRs (red) onto the CDR3α loop (blue, replaced residues).

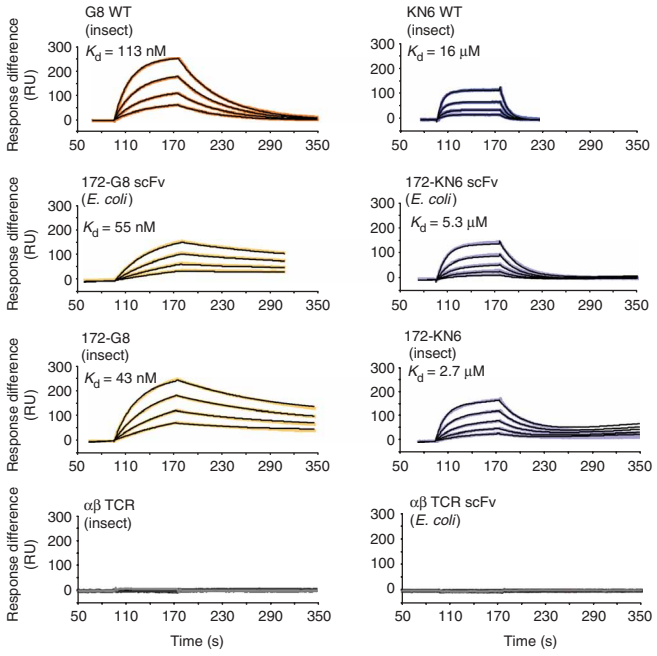

Figure 3 CDR3δ grafted into the αβ TCR retains wild-type affinity for T10 and T22 ligands. Surface plasmon resonance measurements of the binding of T22 to wild-type (WT) full-length G8 γδ TCR (top left) or KN6 γδ TCR (top right) expressed in insect cells; to fusions of the CDR3δ loops of G8 (middle left) or KN6 (middle right) with the 172 αβ TCR single-chain Fv construct (scFv) expressed in *E. coli* (second row) or with full-length 172 expressed in insect cells (third row); or to wild-type full-length 172 αβ TCR expressed in insect cells (bottom left) or the 172 αβ TCR single-chain Fv construct expressed in *E. coli* (bottom right). RU, resonance units. Data are representative of one experiment.

the TCRs) superimposed closely in terms of the register of the polypeptide chain and distance between the residues at the bases of the respective loops (**Supplementary Fig. 1**). The CDR3α of 172.10 is a short, tight turn; we replaced the Asn95-Ser96-Gly97 sequence at the apex of the loop with the respective CDR3δ sequence (**Fig. 2** and **Supplementary Fig. 1**). The CDR3δ loops of G8 and KN6 represent two of the more divergent motifs in the population of TCRs that recognize T22 (**Fig. 2**). Both include a W…EGYEL motif; however, the spacing between the 'W' and 'EGYEL' portions differs: G8 has a three–amino acid residue spacer, whereas KN6 has no spacer.

We used wild-type soluble full-length γδ TCR heterodimers expressed in insect cells to measure the affinity between wild-type TCRs and ligands (**Fig. 3**). To control for artifacts that might be introduced by differences in constructs and expression systems, we expressed the G8 and KN6 CDR3δ-172.10 fusion constructs both in *Escherichia coli* as single-chain Fv constructs (the form of 172.10 that was crystallized) and in insect cells as full-length ectodomain heterodimers connected to leucine zippers. We engineered T22 to contain a carboxy-terminal site-specific biotinylation sequence, which allowed orientation-specific immobilization on streptavidin Biacore chips. We immobilized approximately 250 response units of biotinylated T22 on the chip surface. The wild-type and fusion TCRs were flowed as analyte and we calculated the affinities (assessed as dissociation constant (K_d)) of wild-type G8 and KN6 to be about 100 nM and 15 μM, respectively (**Fig. 3**), which indicated that wild-type G8 and KN6, despite sharing a common but nonidentical CDR3δ motif, bind T22 with very different affinities and kinetics. Each fusion protein specifically bound to T22 (although wild-type 172.10 did not bind) with slightly higher affinity than did its wild-type counterpart (about 50 nM and 4 μM for the G8-172.10 and KN6-172.10 fusion proteins, respectively; **Fig. 3**). These results demonstrated that the CDR3δ loop is the main recognition determinant of the G8 and KN6 TCRs and thus that this loop is probably dominant in the recognition of T22 by other γδ TCRs bearing this motif. The finding that the affinities of the fusion proteins were higher than those of wild-type TCRs suggests that the CDR1 and/or CDR2 loops, or the scaffold, of the wild-type γδ TCRs may impose a barrier to T22 binding and that the fusion proteins essentially unmasked the 'naked' affinity of each of these CDR3δ sequences in an uninhibited context. In this way, the surrounding structural context of CDR3δ can sensitively exert a modulatory effect on the affinity of each γδ TCR for T22 by exerting more or less of an inhibitory effect.

Energetically distinct modes of CDR3δ binding

The 100-fold difference in affinity in the binding of the G8 and KN6 CDR3δ loops to T22 (as shown by both wild-type and fusion TCR measurements) and the different sequence contexts of the shared W…EGYEL motif raises the issue of whether these two divergent loops bind to T22 in similar or distinct ways. To address that, we did alanine-scanning mutagenesis of the CDR3δ loops of these two TCRs to determine the energetically critical residues involved in T22 binding. We did surface plasmon resonance as in the fusion experiments,

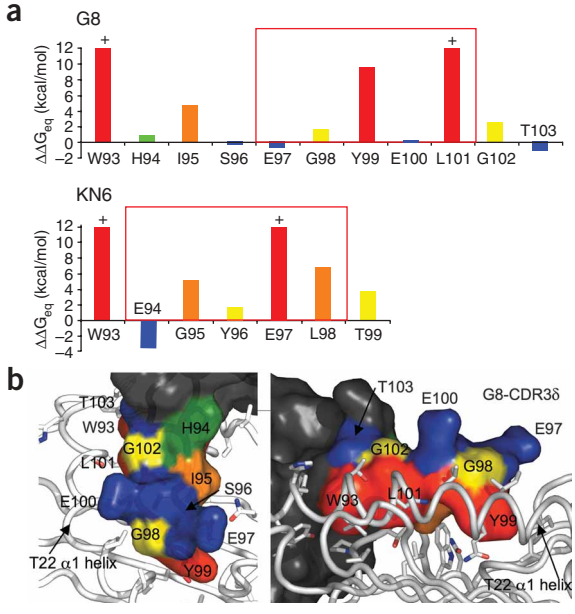

Figure 4 Heterogeneous energetic 'landscapes' of the interactions of G8 and KN6 CDR3δ with T10 and T22. (**a**) Alanine-scanning mutagenesis of the G8 (top) and KN6 (bottom) CDR3δ loops. Horizontal axis, one-letter amino acid designations and positions; +, substitutions resulting in binding below the limit of detection. Bar colors (according to the visual spectrum) indicate the effect of the substitution on binding; red indicates a large ΔΔG 'penalty' on binding (greatest energetic change), and blue indicates little or no ΔΔG 'penalty'. Red boxes outline the conserved EGYEL motif shared by G8 and KN6. $\Delta\Delta G_{eq}$, ΔΔG at equilibrium. Data are representative of one experiment. (**b**) The interface between the G8 γδ TCR and T22 (ref. 1), shown from above (left) and from the side (right), with the residues of the CDR3δ loop in colors as described in **a**, according to their energetic contribution to binding.

Table 1 Allelic variants of T10 and T22

	α1 and α2 domains				α3 domain				G8 γδ stimulation
	35	58	89	124	183	191	196	213	
T22 and $T10^b$	R	D	M	P	D	R	E	I	+++++
$T10^d$	L	G	V	H	E	H	A	L	+

Positions of amino acid differences between allelic variants of T10 and T22; far right, reactivity of the G8 hybridoma to the variants (+, slightly reactive; +++++, very reactive).

with T22 immobilized on the chip surface and each mutant flowing as analyte. For the G8 CDR3δ loop, the residues with the greatest energetic change when substituted with alanine corresponded well with the residues that contacted the T22 surface, as seen in the three-dimensional structure of G8 in complex with T22 (**Fig. 4**). In particular, Trp93, Tyr99 and Leu101 most profoundly influenced free energy (substitution of Trp93 and Leu101 decreased binding to undetectable), whereas the remaining residues of the loop exerted either a moderate effect (such as Ile95, which also contacts T22, and Gly98 and Gly102) or little to a negative effect (His94, Ser96, Glu97, Glu100 and Thr103).

Unexpectedly, alanine scanning of the KN6 CDR3δ loop identified considerable differences in energetically important residues. Whereas Trp93 was also critical for the binding of KN6 to T22, other residues energetically critical for binding of the KN6 CDR3δ loop to T22 seemed to have different energetic functions in G8 (**Fig. 4a**). Glu97 was required for KN6 binding, whereas it had essentially no effect on the binding of G8 to T22. Conversely, Tyr99 was critical for G8 binding, but the KN6 Tyr residue had only a moderate effect on the association of KN6 with T22. These findings provide evidence that the γδ TCRs that bind to T22, although they recognize this ligand almost exclusively through a shared, simple motif (W…EGYEL), can establish an interface with the ligand in very different ways.

Allele-specific γδ TCR binding

To understand the effect of allelic variation in T22 and T10 on γδ TCR binding and γδ T cell stimulation, we measured the affinity of the binding of G8 to T22 and $T10^b$, which strongly stimulated G8 γδ TCR^+ cells, and to $T10^d$, which weakly stimulated G8 γδ TCR^+ cells (**Table 1**). To do this, we expressed the G8 γδ TCR and each ligand in insect cells using a baculovirus expression system. We engineered the TCR with a specific biotinylation sequence at the carboxyl terminus that allowed orientation-specific immobilization on a streptavidin chip. We flowed purified T22, $T10^b$ and $T10^d$ as analyte at concentrations varying from 31.25 nM to 250 nM and measured the 'on rate' and 'off rate' using these sensograms (**Fig. 5**). We fit curves with a 1:1 Langmuir binding and calculated binding affinity (as K_d). G8 bound to its strongly stimulatory ligands T22 and $T10^b$ with affinities of approximately 70 nM and 80 nM, respectively (**Fig. 5** and **Table 2**), similar to values calculated in published studies[24] using bacterially expressed and refolded T22. Unexpectedly, G8 also bound to $T10^d$, a much weaker (10% potency) agonist than T22 even when presented in high concentrations. The affinity of G8 for $T10^d$ was approximately 10% that of G8 for T22; although G8 bound T22 and $T10^d$ with similar association rates, G8 bound $T10^d$ with a tenfold higher dissociation rate (**Fig. 5** and **Table 2**).

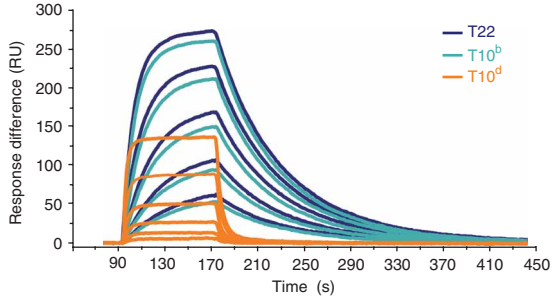

Figure 5 The G8 γδ TCR binds to strong and weak stimulatory ligands with different affinity. Surface plasmon resonance measurements of the binding of T22, $T10^b$ and $T10^d$ to the G8 γδ TCR (K_d and association and dissociation rates, **Table 2**). Data are representative of three experiments.

To determine the amino acid positions responsible for the strong or weak stimulatory activity of the distinct G8 ligands, we generated a series of gain-of-function and loss-of-function mutants of T22, $T10^b$ and $T10^d$. We examined only those amino acids that differed between the strong (T22 and $T10^b$) and weak ($T10^d$) ligands (**Fig. 6**). We generated point substitutions of such residues located in the α1 and α2 domains because according to published complex structure and functional data[1,31] these residues were most likely to affect recognition by the G8 TCR. For simplicity, we substituted all relevant amino acids in the α3 domain in a single molecule. We expressed mutant ligands in insect cells, purified them from supernatants and used them for assays of surface plasmon resonance (as described above) and stimulation of the G8 γδ T cell hybridoma.

Four of the five T22 and $T10^d$ point mutants were very similar to wild-type molecules in terms of affinity and stimulatory capacity (**Figs. 6** and **7a**). However, molecules with a point substitution at position 124 (a histidine in place of a proline (P124H) in T22 and a proline in place of a histidine (H124P) in $T10^d$) reversed the affinity and stimulatory capacity of T22 and $T10^d$ (**Figs. 6**, **7a**). The position of these substitutions is at the edge of the binding interface in the complex structure of G8 and T22 (ref. 1). The proline forms a main-chain hydrogen bond with the side chain of Trp93 of CDR3δ, as well as van der Waals contacts with the main chain at the apex of CDR1δ by a 'knob-in-holes' type of interaction. The introduction of a histidine in this position would alter this contact between T22 (and presumably $T10^b$) and the TCR, as the main chain would be distorted after removal of a proline and a histidine side chain would probably be too bulky to be accommodated in this tightly packed interface (**Fig. 7b**). As indicated by the comparison of the kinetics of binding of T22, $T10^b$ and $T10^d$ (**Fig. 5**), the difference in binding of the G8 TCR to wild-type T22 and its binding to the P124H T22 mutant was due almost exclusively to a higher off rate approaching that of $T10^d$ (**Fig. 6**).

To test whether the substitutions affected the stability of the T22 and $T10^d$ structures, we did circular dichroism studies of each mutant to determine their stability at 37 °C, the physiological temperature used for the stimulation studies. The melting temperature values for the mutants, although they differed slightly between the T22 and $T10^d$ alleles, did not correlate with the observed differences in stimulatory

Table 2 Binding kinetics of G8 to T22, $T10^b$ and $T10^d$

	K_d	K_{on} (1/ms)	K_{off} (1/s)
T22	67 nM	2.5×10^5	1.7×10^{-2}
$T10^b$	81 nM	2.1×10^5	1.7×10^{-2}
$T10^d$	842 nM	2.1×10^5	1.7×10^{-1}

Binding kinetics of the G8 γδ TCR to the highly stimulatory alleles T22 and $T10^b$ and the weakly stimulatory allele $T10^d$. K_{on}, on rate; K_{off}, off rate.

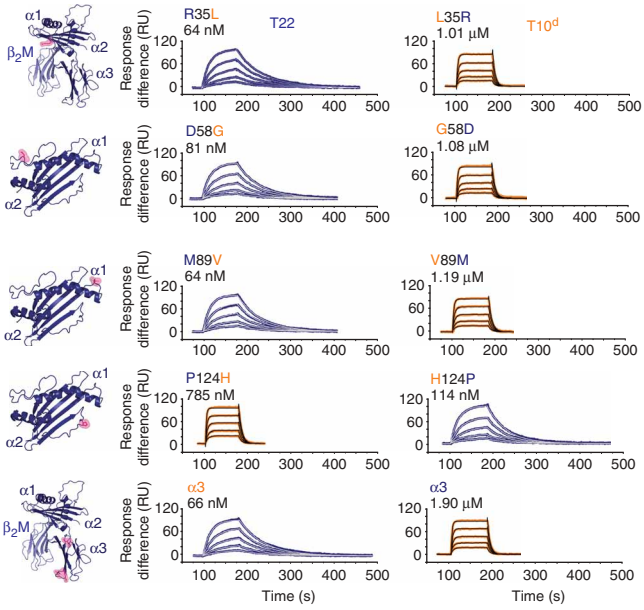

Figure 6 Substitutions responsible for differential G8 γδ TCR binding and stimulation by T22 and T10^b versus T10^d. Surface plasmon resonance measurements of the binding of G8 γδ TCR to T22 (left) and T10^d mutants (right). Blue letters, T22 wild-type residues; orange letters, T10^d wild-type residues. Top left, position of each point substitution and the corresponding calculated affinity (K_d). Left margin, position of each point substitution in the structure of T22 (ref. 49). Data are representative of two experiments.

capacity (**Fig. 7c** and **Supplementary Fig. 2** online). Most notable were the mutants with point substitution at position 124, which despite their distinct stimulatory capacity closely maintained the melting temperatures of their wild-type counterparts. These experiments confirmed that the difference in stimulatory capacities of the mutants was due to the effect of the single point substitution and not to disruption of the secondary structure or stability of the structural backbone. These data collectively show that a single amino acid polymorphism at position 124 modulates the recognition of T22 and T10 molecules by the G8 γδ TCR.

DISCUSSION

The molecular mechanisms by which γδ TCRs engage ligands still remain largely unknown for most γδ TCR–ligand systems. The three-dimensional structure of the G8 γδ TCR in complex with the MHC class Ib molecule T22 (ref. 1) has shown that G8, instead of using an assemblage of many CDR loops to engage ligand, as is usual for interactions between αβ TCRs and peptide-MHC[15] or antibody and antigen[32], bound T22 almost exclusively through its CDR3δ loop with only minor contacts from other CDR loops. Although some TCR-peptide-MHC complexes[33,34] and antibody-antigen complexes[35,36] show a preponderance of interaction through CDR3 regions, the extent of involvement of CDR3δ in the G8-T22 complex and the focus of this interaction on a six–amino acid motif (W…EGYEL) in CDR3δ are highly unusual. In fact, the most similar structural analog is that of the single-chain shark antibodies (IgNAR), which have been shown to bind lysozyme through a long CDR3 that penetrates a 'canyon' on the antigen surface[37].

Here we have shown by grafting experiments that the main recognition determinant of the G8 and KN6 γδ TCRs for T22 is their CDR3δ loops. The ability to recapitulate reactivity through a single CDR loop has to our knowledge not been reported before for TCRs or antibodies and suggests that this recognition process has 'innate-like' features, as most of these residues are encoded by germline fragments rather than through the diversifying P- and N-nucleotide variation that encodes many of the CDR3 contact residues in αβ TCR–peptide–MHC and antibody-antigen complexes. Notably, however, the affinity of this germline segment for T22 is modulated by the P- and N-nucleotide variation bracketing the motif. The G8 γδ TCR, cloned from an alloreactive T cell line derived from a BALB/c (H-2^d) homozygous nude mouse stimulated with irradiated B10.BR (H-2^k, T22-positive) splenocytes[38], bound T22 with 100-fold greater affinity than did the KN6 γδ TCR, of syngenic origin. Our ability to 'sample' this range of affinities of γδ TCRs for T22 was probably due to their allogeneic versus syngeneic origins, as other syngeneic γδ TCRs specific for T22 also bind with affinities lower than that of G8 (ref. 28). Unexpectedly, our alanine-scanning mutagenesis of the CDR3δ loops of G8 and KN6, which differ in the length and 'spacer' amino acids between the W and EGYEL portions of the motif, suggested that recognition of T22 has an additional layer of

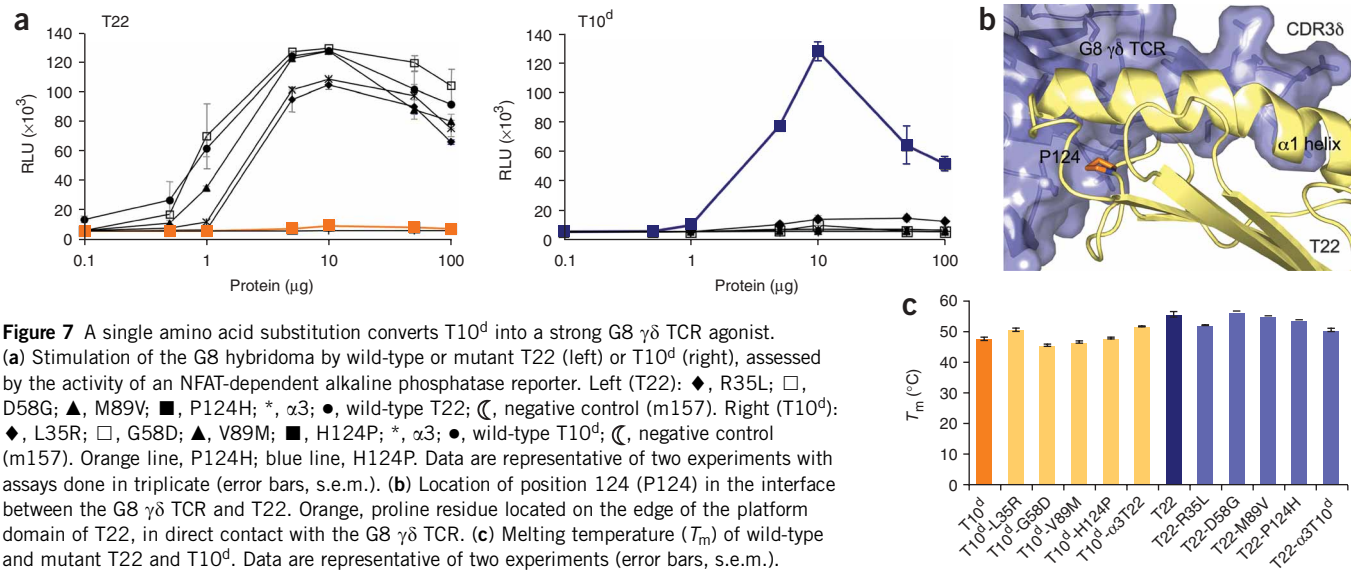

Figure 7 A single amino acid substitution converts T10^d into a strong G8 γδ TCR agonist. (**a**) Stimulation of the G8 hybridoma by wild-type or mutant T22 (left) or T10^d (right), assessed by the activity of an NFAT-dependent alkaline phosphatase reporter. Left (T22): ◆, R35L; □, D58G; ▲, M89V; ■, P124H; *, α3; ●, wild-type T22; ℄, negative control (m157). Right (T10^d): ◆, L35R; □, G58D; ▲, V89M; ■, H124P; *, α3; ●, wild-type T10^d; ℄, negative control (m157). Orange line, P124H; blue line, H124P. Data are representative of two experiments with assays done in triplicate (error bars, s.e.m.). (**b**) Location of position 124 (P124) in the interface between the G8 γδ TCR and T22. Orange, proline residue located on the edge of the platform domain of T22, in direct contact with the G8 γδ TCR. (**c**) Melting temperature (T_m) of wild-type and mutant T22 and T10^d. Data are representative of two experiments (error bars, s.e.m.).

complexity. Our results have shown that the residues composing the shared sequence motif contribute differently to the interaction of G8 and KN6 with T22, which indicates that different amino acids in these loops, or 'registers', are used for T22 recognition. It is difficult to understand why or how a shared motif would be used in different energetic and structural contexts by different TCRs recognizing an identical ligand. However, it is apparent that in both cases, the TCR reactivity is endowed by CDR3δ alone, so both loops share the same level of structural autonomy. The distinct T22-binding energetics of the W…EGYEL motif in different γδ TCRs could endow these receptors with additional flexibility in ligand recognition that would serve to enhance the repertoire of ligands recognized.

More broadly, we do not know of another example from a protein-protein interaction system, in the immune system or otherwise, in which transfer of a single contiguous polypeptide loop sequence from one protein to a naive protein transfers wild-type affinity to the hybrid protein. This suggests an evolutionary focusing of the binding energetics on a single short polypeptide stretch. A comparable example is that of the *in vitro* evolution of antibodies and/or TCR by phage or yeast display methods. There are examples in which randomization and selection of single CDR loops results in substantially higher affinity of the antibody[39] or TCR[40] for its cognate ligand. However, even in those cases, the other CDR loops contribute to and are necessary for ligand recognition. For αβ TCRs, CDR grafting has so far not succeeded in reconstituting reactivity to a naive TCR, even when multiple CDRs are replaced in parallel[41]. In cases of antibodies, in which many CDR loops are transferred from mouse to human frameworks for antibody 'humanization', considerable protein engineering of the junctional and framework residues is usually needed to reconstitute the affinity of the mouse monoclonal antibody in the humanized antibody[42].

What might be the functional implications of such an autonomous and focused binding determinant? Our observations might indicate that in this case, a germline-encoded element has a coevolved bias for its ligand, similar to the bias of the αβ TCR V segment for MHC[43,44]. Thus, as there is only a fixed number of germline-encoded γδ TCR elements, the repertoire of γδ TCR ligands might be very limited. The ligand specificities of the other germline elements remain unknown. However, we must also introduce the caveat that the G8-T22 system could be unusual, even for γδ TCRs, and that other γδ TCRs may more closely resemble the more canonical antigen receptor interactions in which specificity is achieved through CDR3 recombination and a contribution of multiple CDR loops.

The MHC class Ib molecules T10 and T22 are polymorphic in their genomic and allelic forms, which suggests that there is selection to alter their molecular makeup. This is not unusual in ligands of the immune response, as these molecules are often targets of pathogen downregulation or modulation during immunoevasion[45] and therefore are rapidly evolving. The polymorphisms beyond those required for the function of the protein might be due to a molecular 'arms race' with the pathogen, affecting how microbial proteins interact with these ligands. To compensate for that, host receptors that recognize these ligands are either polymorphic (such as killer immunoglobulin-like receptors and Ly49 receptors) or have an intrinsic diversifying process (such as somatically rearranged TCRs and B cell antigen receptors).

We have identified a single polymorphism (P124H) that modulated the kinetics and stimulatory capacity of the T10 and T22 molecules with the G8 γδ TCR and have shown that other polymorphisms in these ligands were not important in G8 engagement and did not affect ligand stability, as assessed by circular dichroism at physiological temperatures. The substitution of histidine for proline at position 124, located at the edge of T22's docking site, would introduce a steric 'clash' for G8 binding, as is evident from the three-dimensional structure of G8 in complex with T22 (ref. 1). Only weak van der Waals contacts are made with proline 124 by the CDR1 and hypervariable 4 loops and, as an indication that this contact is probably nonspecific, there are evident shifts of these contacts by comparison of the two complexes in the asymmetric unit. That observation, along with the fact that T22-reactive γδ TCRs use a variety of V_δ domains (and, in some cases, V_α domains) in their rearrangement, suggests that considerable binding specificity is not contributed by CDR1 or hypervariable 4. Instead, as suggested by our CDR3δ fusion experiments, the CDR1 and hypervariable 4 loops may exert an inhibitory affect on the binding of G8 and KN6, as transfer of the CDR3δ loops from these TCRs into a naive background resulted in higher binding affinity. Thus, the variation in the T10 and T22 ligands, possibly a consequence of pathogen-driven selection, seems to be accommodated by the structural and sequence adaptability intrinsic to their rearranged receptors. We have shown one example of a ligand polymorphism with a profound effect on TCR engagement and stimulation; specific details of ligand discrimination await study of TCRs specific for other allelic forms of these ligands.

The adaptability of receptors to rapidly evolving or new ligands is the hallmark of the unique process of somatic variable-diversity-joining rearrangement. The intrinsic variation of these receptors and a carefully 'tuned' selection process allows αβ TCRs to discriminate between allelic forms of MHC molecules and the variable peptides they bind and present and allows antibodies to distinguish between new protein and nonprotein ligands such as those introduced during bacterial or viral infection. We have shown here that recognition of T22 and T10 by the γδ TCR can be modulated by allelic variation, that the CDR3δ loop is an autonomous determinant of ligand recognition and that the shared amino acid motif in this loop can have its ligand affinity 'tuned' by different surrounding contexts of CDR3δ sequence.

METHODS

Protein expression and purification. $T10^b$, $T10^d$ and T22 were expressed and purified as described[1]. The soluble ectodomains of these proteins were engineered for secretion into the supernatants of Hi5 insect cells by the baculovirus expression system. Six-histidine tags were placed at the carboxyl terminus for nickel agarose purification. Supernatants of infected cells were collected and concentrated and were exchanged with HBS buffer (10 mM HEPES, pH 7.2, 150 mM NaCl and 0.02% (wt/vol) azide), with nickel agarose (nickel–nitrilotriacetic acid; Qiagen) added at a dilution of about 1/100–1/50, depending on protein expression. Imidazole, pH 8, was added to a concentration of about 20 mM to reduce nonspecific binding of protein to the nickel–nitrilotriacetic acid. Proteins were eluted from the nickel agarose resin by the addition of 200 mM imidazole in HBS. Proteins were further purified by gel filtration over a Superdex S200 size-exclusion column (GE Healthcare). Full-length G8 and KN6 were expressed as described for G8, with the baculovirus expression system (described above). They were fused to acidic and basic leucine zippers containing six-histidine tags at their carboxyl termini to aid in the proper formation of heterodimers and disulfide pairing of the γ- and δ-chains. Placement of 3C rhinovirus protease sites between the TCR and zippers allowed easy removal of the zippers and histidine tags after nickel agarose purification (as described above for T10 and T22). Protease-digested TCRs were further purified by gel filtration over a Superdex S200 size-exclusion column (GE Healthcare). Proper disulfide-linked formation of dimers by the TCRs was assessed by nonreducing and reducing SDS-PAGE, which showed 100% efficiency of dimer formation by the purified proteins. The G8 and KN6 fusion proteins were engineered by superposition of the G8 protein structure[1] on the 172 protein structure[30] with the program Pymol (Delano Scientific) to best determine the point at which fusion of the CDR3δ loop with the CDR3α

loop of 172 should begin and end. The α-chain was chosen as the fusion partner because of its close homology with the δ-chain (for example, some V_α domains are used in place of V_δ in γδ TCR rearrangement; G8, for example, uses V_α11.3). To maintain the register of amino acids, the CDR3α loop (Asn-Ser-Gly) was swapped with the CDR3δ loop, starting with the Trp residue and ending with the Thr residue (**Fig. 2**). Fusions were made with overlapping PCR primers encoding the motifs of the G8 and KN6 loops. Sequences of all clones were verified. Expression constructs were made for insect expression (full-length, including variable and constant domains of both chains, producing disulfide-linked, heterodimeric ectodomains) and *E. coli* (single chain, containing variable domains only, linked with a 15–amino acid glycine-serine linker[30]). Full-length fusion TCRs were expressed with the baculovirus expression system as described above for G8 and KN6, and single-chain fusion TCRs were expressed by periplasmic secretion[46]. All proteins were purified by nickel agarose chromatography and gel filtration over a Superdex S200 column (GE Healthcare). Alanine mutants were generated by overlapping PCR with the G8 and KN6 single-chain Fv TCR fusion proteins as templates. The sequence of each mutant was verified and mutants were expressed as described above for the fusion proteins by periplasmic secretion in *E. coli*. All purification proceeded as described above. All biotinylated constructs were engineered with a site-specific biotinylation sequence (GLNDIFEAQKIEWHE; Avidity) at the carboxyl terminus to allow orientation-specific immobilization on a strepavidin Biacore chip (details below in the section describing measurement of surface plasmon resonance). A 3C rhinovirus protease site and six-histidine tag were placed after the biotinylation site for purification with nickel agarose chromatography (nickel–nitrilotriacetic acid; Qiagen). After purification with nickel–nitrilotriacetic acid, the six-histidine tag was removed by digestion overnight at 4 °C with 3C-rhinovirus protease. These constructs were biotinylated with BirA biotin protein ligase (Avidity) according to the manufacturer's protocols. Biotinylated products were purified over a Superdex S200 column (GE Healthcare) in HBS.

Circular-dichroism analysis. Circular-dichroism data were collected on an Aviv 202-01 spectrometer (Aviv Biomedial) equipped with a thermoelectric unit with a cell with a path length of 1 mm. Protein samples were at a concentration of 15 μM in buffer containing 20 mM sodium phosphate, pH 7.1, and 25 mM NaCl. Protein concentrations were determined by ultraviolet spectrophotometry. Thermal melting was monitored at 220 nm. Data were collected every 2 °C with an equilibration time of 20 min and an averaging time of 20 s. The equilibration time for the thermal denaturation was chosen on the basis of a kinetic scan. In the kinetic scan, thermal unfolding was initiated by a temperature increase to 50 °C (approximate midpoint of the thermal denaturation) and the circular-dichroism signal was monitored continuously for 1 h. The protein seemed to reach equilibrium in approximately 15 min. The melting temperature was determined by fitting of the melting curves to a two-state model as described[47].

Surface plasmon resonance. All surface plasmon resonance was measured at 25 °C on a Biacore 3000 with streptavidin chips (SA chips; Biacore) used for immobilizing ligand. HBS-P buffer (10 mM HEPES, pH 7.4, 150 mM NaCl and 0.005% (vol/vol) surfactant P20; Biacore) was used for all measurements. In each experiment, approximately 200–400 response units of biotinylated ligand were immobilized on the chip, followed by blockade for 1 min with free biotin (100 nM). Analyte concentrations ranged from 10 μM to 0.0625 μM depending on the experiment. Sensograms were fit locally with Biacore 3000 analysis software (BIAevaluation Version 3.1) using 1:1 Langumuir binding. On and off rates were determined from those concentration-dependent fits and K_d was calculated. The change in Gibbs free energy (ΔΔG) was calculated with a Gibbs free energy equation incorporating differences between mutant and wild-type as follows: $\Delta\Delta G = RT\ln(K_{dMUT} / K_{dWT})$, where R is the gas constant, T is the temperature in Kelvin, K_{dMUT} is the mutant dissociation constant and K_{dWT} is the wild-type dissociation constant.

Cell stimulation. Cell stimulation was analyzed with G8 hybridoma transfected with an alkaline phosphatase gene reporter under control of the transcription factor NFAT reporter as described[48]. Cells were maintained in RPMI 1640 medium supplemented with 10% (vol/vol) FCS, L-glutamine and the antibiotics penicillin and streptomycin ('RPMI complete'). A volume of 100 μl of insect-expressed wild-type and mutant T22 and $T10^d$ diluted in PBS, pH 7.2, was plated at concentrations varying from 100 μg/ml to 0.1 μg/ml in a flat-bottomed polystyrene tissue culture plate, followed by incubation overnight at 4 °C. The next day, plates were washed with PBS, and 100 μl G8 hybridoma, at a density of 1×10^6 cells per ml of RPMI 1640 medium supplemented with 10% (vol/vol) FCS, was added to each well, followed by incubation for 24 h at 37 °C in an incubator at 5% CO_2. Endogenous phosphatase activity was inactivated by incubation of the plate for 1 h at 65 °C. A volume of 100 μl 4-methylumbelliferyl palmitate (Sigma) was added, followed by incubation overnight at 37 °C. Fluorescence was measured with an excitation wavelength of 360 nm and an emission wavelength of 440 nm. All measurements were made in triplicate.

Note: Supplementary information is available on the Nature Immunology website.

ACKNOWLEDGMENTS

Supported by the National Institutes of Health (R01 AI65504 to K.C.G. and R01 AI073922 to E.J.A.) and the Howard Hughes Medical Institute (K.C.G.).

AUTHOR CONTRIBUTIONS

E.J.A. designed, did and analyzed experiments; P.S. designed, did and analyzed circular dichroism experiments; S.S. assisted in cell-stimulation assays; Y.-H.C. provided intellectual insight; and E.J.A. and K.C.G. provided intellectual guidance and prepared the manuscript.

Published online at http://www.nature.com/natureimmunology/
Reprints and permissions information is available online at http://npg.nature.com/reprintsandpermissions/

1. Adams, E.J., Chien, Y.H. & Garcia, K.C. Structure of a γδ T cell receptor in complex with the nonclassical MHC T22. *Science* **308**, 227–231 (2005).
2. Allison, T.J., Winter, C.C., Fournie, J.J., Bonneville, M. & Garboczi, D.N. Structure of a human γδ T-cell antigen receptor. *Nature* **411**, 820–824 (2001).
3. Battistini, L. *et al.* Phenotypic and cytokine analysis of human peripheral blood γδ T cells expressing NK cell receptors. *J. Immunol.* **159**, 3723–3730 (1997).
4. Spada, F.M. *et al.* Self-recognition of CD1 by γ/δ T cells: implications for innate immunity. *J. Exp. Med.* **191**, 937–948 (2000).
5. Ferrick, D.A. *et al.* Differential production of interferon-γ and interleukin-4 in response to Th1- and Th2-stimulating pathogens by γδ T cells *in vivo*. *Nature* **373**, 255–257 (1995).
6. Wen, L. *et al.* Primary γδ cell clones can be defined phenotypically and functionally as Th1/Th2 cells and illustrate the association of CD4 with Th2 differentiation. *J. Immunol.* **160**, 1965–1974 (1998).
7. Brenner, M.B. *et al.* Identification of a putative second T-cell receptor. *Nature* **322**, 145–149 (1986).
8. Fisch, P. *et al.* Gamma/delta T cell clones and natural killer cell clones mediate distinct patterns of non-major histocompatibility complex-restricted cytolysis. *J. Exp. Med.* **171**, 1567–1579 (1990).
9. Wright, A. *et al.* Cytotoxic T lymphocytes specific for self tumor immunoglobulin express T cell receptor δ chain. *J. Exp. Med.* **169**, 1557–1564 (1989).
10. Jameson, J. *et al.* A role for skin γδ T cells in wound repair. *Science* **296**, 747–749 (2002).
11. Brandes, M., Willimann, K. & Moser, B. Professional antigen-presentation function by human γδ T cells. *Science* **309**, 264–268 (2005).
12. Kapp, J.A., Kapp, L.M. & McKenna, K.C. γδ T cells play an essential role in several forms of tolerance. *Immunol. Res.* **29**, 93–102 (2004).
13. De Libero, G. Tissue distribution, antigen specificity and effector functions of γδ T cells in human diseases. *Springer Semin. Immunopathol.* **22**, 219–238 (2000).
14. Garcia, K.C. & Adams, E.J. How the T cell receptor sees antigen–a structural view. *Cell* **122**, 333–336 (2005).
15. Rudolph, M.G. & Wilson, I.A. The specificity of TCR/pMHC interaction. *Curr. Opin. Immunol.* **14**, 52–65 (2002).
16. Davies, D.R. & Cohen, G.H. Interactions of protein antigens with antibodies. *Proc. Natl. Acad. Sci. USA* **93**, 7–12 (1996).
17. Porcelli, S. *et al.* Recognition of cluster of differentiation 1 antigens by human CD4–CD8-cytolytic T lymphocytes. *Nature* **341**, 447–450 (1989).
18. Schild, H. *et al.* The nature of major histocompatibility complex recognition by γδ T cells. *Cell* **76**, 29–37 (1994).
19. Weintraub, B.C., Jackson, M.R. & Hedrick, S.M. Gamma delta T cells can recognize nonclassical MHC in the absence of conventional antigenic peptides. *J. Immunol.* **153**, 3051–3058 (1994).
20. Groh, V., Steinle, A., Bauer, S. & Spies, T. Recognition of stress-induced MHC molecules by intestinal epithelial γδ T cells. *Science* **279**, 1737–1740 (1998).
21. Scotet, E. *et al.* Tumor recognition following Vγ9Vδ2 T cell receptor interactions with a surface F1-ATPase-related structure and apolipoprotein A-I. *Immunity* **22**, 71–80 (2005).
22. Johnson, R.M. *et al.* A murine CD4-, CD8- T cell receptor-γδ T lymphocyte clone specific for herpes simplex virus glycoprotein I. *J. Immunol.* **148**, 983–988 (1992).

23. Elliott, J.F., Rock, E.P., Patten, P.A., Davis, M.M. & Chien, Y.H. The adult T-cell receptor δ-chain is diverse and distinct from that of fetal thymocytes. *Nature* **331**, 627–631 (1988).
24. Crowley, M.P. *et al.* A population of murine γδ T cells that recognize an inducible MHC class Ib molecule. *Science* **287**, 314–316 (2000).
25. Bluestone, J.A., Cron, R.Q., Cotterman, M., Houlden, B.A. & Matis, L.A. Structure and specificity of T cell receptor γ/δ on major histocompatibility complex antigen-specific $CD3^+$, $CD4^-$, $CD8^-$ T lymphocytes. *J. Exp. Med.* **168**, 1899–1916 (1988).
26. Bonneville, M. *et al.* Recognition of a self major histocompatibility complex TL region product by γδ T-cell receptors. *Proc. Natl. Acad. Sci. USA* **86**, 5928–5932 (1989).
27. Ito, K. *et al.* Recognition of the product of a novel MHC TL region gene (27b) by a mouse γδ T cell receptor. *Cell* **62**, 549–561 (1990).
28. Shin, S. *et al.* Antigen recognition determinants of γδ T cell receptors. *Science* **308**, 252–255 (2005).
29. Li, H. *et al.* Structure of the Vδ domain of a human γδ T-cell antigen receptor. *Nature* **391**, 502–506 (1998).
30. Maynard, J. *et al.* Structure of an autoimmune T cell receptor complexed with class II peptide-MHC: insights into MHC bias and antigen specificity. *Immunity* **22**, 81–92 (2005).
31. Moriwaki, S., Korn, B.S., Ichikawa, Y., van Kaer, L. & Tonegawa, S. Amino acid substitutions in the floor of the putative antigen-binding site of H-2T22 affect recognition by a γδ T-cell receptor. *Proc. Natl. Acad. Sci. USA* **90**, 11396–11400 (1993).
32. Padlan, E. Anatomy of the antibody molecule. *Mol. Immunol.* **31**, 169–217 (1994).
33. Garboczi, D.N. *et al.* Structure of the complex between human T-cell receptor, viral peptide and HLA-A2. *Nature* **384**, 134–141 (1996).
34. Reiser, J.B. *et al.* A T cell receptor CDR3β loop undergoes conformational changes of unprecedented magnitude upon binding to a peptide/MHC class I complex. *Immunity* **16**, 345–354 (2002).
35. Huang, C.C. *et al.* Structures of the CCR5 N terminus and of a tyrosine-sulfated antibody with HIV-1 gp120 and CD4. *Science* **317**, 1930–1934 (2007).
36. Kodandapani, R., Veerapandian, B., Kunicki, T.J. & Ely, K.R. Crystal structure of the OPG2 Fab. An antireceptor antibody that mimics an RGD cell adhesion site. *J. Biol. Chem.* **270**, 2268–2273 (1995).
37. Stanfield, R.L., Dooley, H., Flajnik, M.F. & Wilson, I.A. Crystal structure of a shark single-domain antibody V region in complex with lysozyme. *Science* **305**, 1770–1773 (2004).
38. Matis, L.A., Cron, R. & Bluestone, J.A. Major histocompatibility complex-linked specificity of γδ receptor-bearing T lymphocytes. *Nature* **330**, 262–264 (1987).
39. Lee, C.V. *et al.* High-affinity human antibodies from phage-displayed synthetic Fab libraries with a single framework scaffold. *J. Mol. Biol.* **340**, 1073–1093 (2004).
40. Holler, P.D. *et al.* In vitro evolution of a T cell receptor with high affinity for peptide/MHC. *Proc. Natl. Acad. Sci. USA* **97**, 5387–5392 (2000).
41. Patten, P.A. *et al.* Transfer of putative complementarity-determining region loops of T cell receptor V domains confers toxin reactivity but not peptide/MHC specificity. *J. Immunol.* **150**, 2281–2294 (1993).
42. Presta, L.G. *et al.* Humanization of an antibody directed against IgE. *J. Immunol.* **151**, 2623–2632 (1993).
43. Feng, D., Bond, C.J., Ely, L.K., Maynard, J. & Garcia, K.C. Structural evidence for a germline-encoded T cell receptor-major histocompatibility complex interaction 'codon'. *Nat. Immunol.* **8**, 975–983 (2007).
44. Huseby, E.S. *et al.* How the T cell repertoire becomes peptide and MHC specific. *Cell* **122**, 247–260 (2005).
45. Hewitt, E.W. The MHC class I antigen presentation pathway: strategies for viral immune evasion. *Immunology* **110**, 163–169 (2003).
46. Maynard, J. *et al.* High-level bacterial secretion of single-chain αβ T-cell receptors. *J. Immunol. Methods* **306**, 51–67 (2005).
47. Minor, D.L. Jr. & Kim, P.S. Measurement of the β-sheet-forming propensities of amino acids. *Nature* **367**, 660–663 (1994).
48. Crowley, M.P., Reich, Z., Mavaddat, N., Altman, J.D. & Chien, Y. The recognition of the nonclassical major histocompatibility complex (MHC) class I molecule, T10, by the γδ T cell, G8. *J. Exp. Med.* **185**, 1223–1230 (1997).
49. Wingren, C., Crowley, M.P., Degano, M., Chien, Y. & Wilson, I.A. Crystal structure of a γδ T cell receptor ligand T22: a truncated MHC-like fold. *Science* **287**, 310–314 (2000).